New BIOTECHNOLOGY 89 (2025) 73–81

Contents lists available at ScienceDirect

New BIOTECHNOLOGY

journal homepage: www.elsevier.com/locate/nbt

Improving PHB production in cyanobacteria: Modeling the optimal light regime for growth

I. Perez Couñago [a,*], J.M. Fernandez Montenegro [a], S. Iglesias Moreira [a], F. Rodriguez Lorenzo [a], M. Placer Lorenzo [a], P. Villar Sola [a], E. Pancorbo González [a], J. Illade Quinteiro [a], L. Herrero Castilla [a], J.A. Álvarez Rodríguez [a], B. Altamira Algarra [b], E. Gonzalez Flo [b], J. Garcia [b], F. Guedes [c], M. Lopez-Garcia [c], S. Muiños-Landin [a]

[a] AIMEN, Technology center, Environmental Technologies Unit/Robotics and Control Unit, Polígono Industrial de Cataboi SUR-PPI-2 (Sector 2) Parcela 3, O Porriño, 36418, Spain

[b] GEMMA-Group of Environmental Engineering and Microbiology, Department of Civil and Environmental Engineering, Escola d'Enginyeria de Barcelona Est (EEBE), Universitat Politècnica de Catalunya-BarcelonaTech, Av. Eduard Maristany 16, Building C5.1, Barcelona, E-08019, Spain

[c] Natural and Artificial Photonic Structures and Devices Group, International Iberian Nanotechnology Laboratory, Braga, 4715-330, Portugal

ARTICLE INFO

Keywords:
Cyanobacteria
Bioplastics
Modeling
Optimization
Light regime

ABSTRACT

The production of bioplastics, such as polyhydroxybutyrate (PHB), using cyanobacteria offers a sustainable alternative to conventional plastics. However, achieving economically viable production requires optimizing biomass growth. This study examined four growth models: Gompertz (empirical growth), Baranyi-Roberts (biologically dependent), Monod (nutrient dependent), and Aiba (irradiance dependent). The results indicate that a light-based model more accurately describes cyanobacterial growth and shows potential for optimizing light regimes. Additionally, an estimator was proposed to assess the potential PHB yield within the given biomass. Experiments were conducted to correlate photosynthetic efficiency with biomass production, providing deeper insights into the effects of light on growth. These findings support the development of optimized cultivation strategies, ultimately improving the economic viability of cyanobacteria-based bioplastics.

1. Introduction

While large-scale plastic production has driven advancements across various industries, it has also resulted in significant environmental costs [1]. Bioplastics, made from renewable resources, have emerged as a sustainable alternative that supports a circular economy, reduces carbon emissions, and lowers toxicity during production and degradation [2]. Polyhydroxy alkanoates (PHAs) have received much attention in the current scenario due to their potential to replace polypropylene (PP) [3]. Cyanobacteria are promising candidates for producing polyhydroxy butyrate (PHB), a type of PHA, as they offer lower production costs, require less cultivation space, and grow faster than many plant organisms [4]. PHB production in cyanobacteria involves inoculum preparation, a growth phase, and the regulation of environmental variables to redirect metabolism to PHB synthesis [5]. Mathematical models play a crucial role in optimizing these processes by estimating biomass growth rates under varying conditions. Through simulation, models guide adjustments to cultivation parameters, offering insights into growth dynamics and metabolic responses, thereby enabling the development of optimized cultivation strategies.

This study focuses on modeling the accumulation of cyanobacterial biomass and estimating PHB yield. We compared four well-established models, each incorporating different variables, to assess the environment influences on these processes. Building on these models, a new model combining irradiance, temperature, and pH was developed, demonstrating the highest accuracy in reproducing laboratory observations and showing potential for providing insights to optimize light regimes. In parallel, experiments were conducted to examine the correlation between biomass and photosynthetic activity, to identify strategies to enhance biomass productivity.

Novelty of this research lies in its integration of model-based insights with experimental data, comparing different models under the same experimental conditions, a comparison that has not been widely explored in the literature. Additionally, we explore the interplay between light, biomass, and photosynthetic activity using PAM-FIS techniques, an area where limited information exists for cyanobacteria. By fine-tuning cultivation strategies and creating favorable conditions for metabolic efficiency, cyanobacterial cultures can be optimized for enhanced PHB production.

* Corresponding author.
E-mail address: ines.perez@aimen.es (I.P. Couñago).

https://doi.org/10.1016/j.nbt.2025.05.005

Available online 17 June 2025

Nomenclature

a_0	Growth retardation coefficient
a	PHB accumulation rate [h^{-1}]
b	PHB degradation rate [$gL^{-1}h^{-1}$]
K_S	Light saturation coefficient [$\mu molm^{-2}s^{-1}$]
K_I	Light inhibition coefficient [$\mu molm^{-2}s^{-1}$]
K_N	Nitrogen saturation coefficient [gL^{-1}]
I	Irradiance [$\mu molm^{-2}s^{-1}$]
lag	Growth retardation coefficient for Gompertz model
$M8$	Microbiome primarily composed of *Synechocystis sp.* and *Synechococcus sp.*
$M11$	Microbiome primarily composed of *Synechococcus sp.* and green algae
N	Concentration of nitrogen [gL^{-1}]
PBR	Photobioreactor
Sy	*Synechocystis sp.*
T	Temperature [°C]
$T1$	Temperature-Driven Model 1
$T2$	Temperature-Driven Model 2
t	time [h]
$\mu(\cdot)$	Specific growth rate [h^{-1}]
μ	Maximum growth rate [h^{-1}]
μ_d	Decay rate [$gL^{-1}h^{-1}$]
X	Biomass concentration [gL^{-1}]
X_0	Initial biomass concentration [gL^{-1}]

2. Materials and methods

2.1. Experimental data

Cyanobacteria were cultured in a 3-liter photobioreactor using BG-11 medium at ambient temperature. pH levels were maintained between 7 and 8 through controlled CO_2 injection. The lighting regimen consisted of 16 h of illumination under cool white fluorescent light at an intensity of 400 PPFD, followed by 8 h of darkness. To evaluate biomass content, a 10 mL sample was extracted from the photobioreactor, and fixed solids were separated by igniting the sample at 550 °C, following the Standard Methods for the Examination of Water and Wastewater [6], which allows for the quantification of volatile suspended solids (VSS). Biomass quantification was conducted daily at 8:00, 12:00, and 15:00, with no sampling on weekends, resulting in 17-hour intervals on weekdays and a maximum interval of 65 h over the weekend. The experimental setup is illustrated in Fig. 1.

Experimental data, detailed in Table 1, was organized into three datasets to address strain differences and potential variations in laboratory conditions:

- Dataset 1 (Synechocystis - AIMEN). Growth data from *Synechocystis sp.* strain R2020, isolated from a wastewater treatment plant using microalgae [7], cultivated at the AIMEN laboratory.
- Dataset 2 (Microbiomes - AIMEN): Growth data for two microbiome types: (i) M11 (primarily composed of *Synechococcus sp.* and green algae) and (ii) M8 (primarily composed of *Synechocystis sp.* and *Synechococcus sp.*, described in [8]), cultivated at the AIMEN laboratory.
- Dataset 3 (Microbiomes - UPC). Growth data for microbiomes M8 and M11, cultivated at the Universitat Politècnica de Catalunya (UPC) laboratory.

PHB data, expressed as the amount of PHB accumulated within the biomass, were collected over a 126-day period from two photobioreactors (PBR-1 and PBR-2) at the UPC laboratory. The data collection process involved a series of growth and accumulation cycles. In the initial growth phases, cultures were supplied with optimal levels of essential nutrients, light, and carbon dioxide to promote robust cellular growth. Following this, cells entered a dark period combined with nutrient deprivation, which triggered PHB accumulation as an energy reserve in response to stress. Once the production of PHB began to stabilize, nutrient replenishment was introduced under illuminated conditions to promote further growth. More details on the strategies employed to stimulate PHB accumulation can be found in [5].

PHB analysis was adapted from the methodology described in [9]. PHB was extracted from the biomass by a digestion procedure prior to gas chromatography (GC) analysis. Briefly, 50 mL of mixed liquor was collected and centrifuged at 4200 rpm for 7.5 min. The samples were then frozen at −80 °C overnight in an ultra-freezer (Arctiko, Denmark) and subsequently freeze-dried for 24 h in a freeze dryer at −110 °C and 0.05 hPa (Scanvac, Denmark). Approximately 3–3.5 mg of freeze-dried biomass were mixed with 1 mL of CH_3OH with H_2SO_4 (20% v/v) and 1 mL of $CHCl_3$ containing 0.05% w/w benzoic acid. The samples were heated for 5 h at 100 °C in a dry-heat thermo-block (Selecta, Spain). After the heating step, the samples were placed in a cold-water bath for 30 min to cool. Subsequently, 1 mL of deionized water was added to the tubes, and they were vortexed for 1 min. The $CHCl_3$ phase was then recovered using a glass pipette and transferred to a chromatography vial containing molecular sieves. Samples were analyzed by GC (7820A, Agilent Technologies, USA) using a DB-WAX 125–7062 column (Agilent Technologies, USA). Helium was used as the carrier gas at a flow rate of 4.5 mL min^{-1}. The injector had a split ratio of 5:1 and a temperature of 230 °C. The FID was set to 300 °C. A standard curve of the co-polymer PHB-HV was used to quantify the PHB content.

2.2. Model development

2.2.1. Model selection

A review of the literature led to the selection of four growth models, each chosen for their different biological foundations. Although other models exist, those selected were chosen primarily for their acceptance in the literature and their computational tractability. Based on this review, the following models were considered the most appropriate for the objectives of the study, providing a framework for capturing key variables influencing cyanobacterial growth that aligns well with the dataset used in this study:

- Mathematical Response - Gompertz Model [10]. The Gompertz curve was adapted to ensure biological relevance, making it a foundational model for cyanobacterial growth.
- Biological Response - Baranyi-Roberts Model [11]. The growth is modeled based on the organism's ability to adapt to the culture medium, focusing on the biological characteristics of cyanobacteria.
- Environmental Response
  - Nutrients - Monod Model [12]. Links growth rate to substrate levels (e.g., nitrogen), addressing nutrient limitation.
  - Light - Aiba Model [13]. Models growth in response to light intensity, incorporating photolimitation and photoinhibition effects.
  - pH. Links growth rate to an optimal pH range, with a decline as pH deviates from this value [7]. This approach was chosen for its simplicity and effectiveness.
  - Temperature: We modeled temperature effects on growth using both a pH-like approach [7] (T1 model) and the Arrhenius equation, which incorporates temperature-dependent parameters [13] (T2 model).

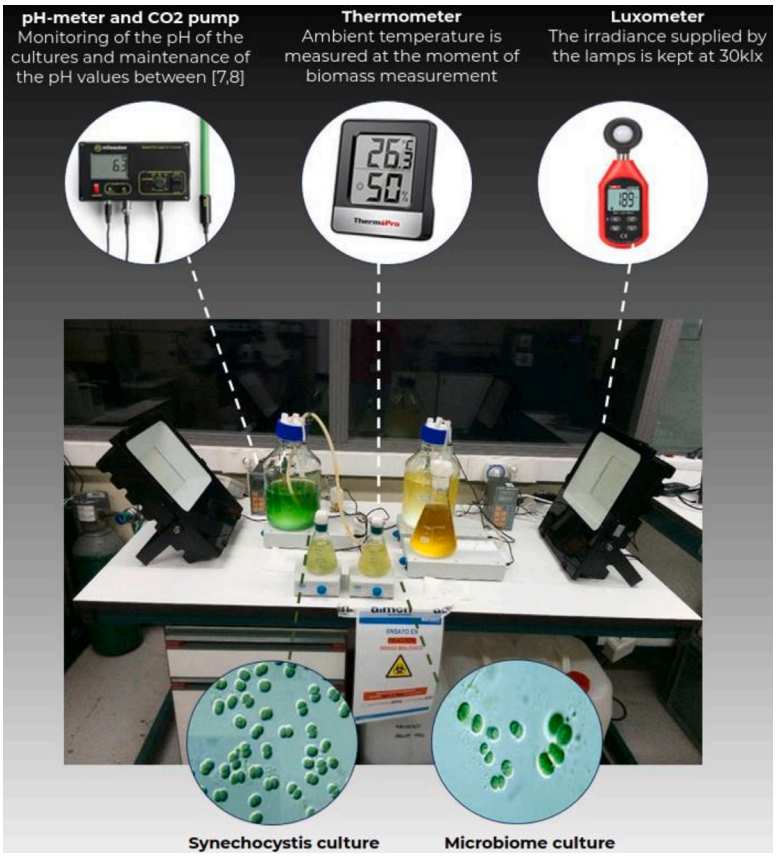

Fig. 1. AIMEN experimental setup for monitoring cyanobacterial growth.

Table 1
Summary of experimental growth data, including dataset ID, strain type, number of experiments (#Exp), and key culture conditions (pH, temperature, nitrogen concentration, and irradiance) for each laboratory.

Lab	Dataset	Strains	#Exp	pH	T [°C]	N [mg/L]	I [PPFD]
AIMEN	1	*Synechocystis sp.*	2	6.80	20.6	25	400
	1	*Synechocystis sp.*	1	6.98	22.0	25	400
	2	M11 microbiome	1	7.05	24.0	2	400
	2	M11 microbiome	1	6.62	24.0	2	400
	2	M8 microbiome	1	7.65	19.8	2	400
UPC	3	M11 microbiome	28	–	35.0	25	400
	3	M11 microbiome	2	–	35.0	50	400
	3	M8 microbiome	10	–	35.0	25	400
	3	M8 microbiome	1	–	35.0	50	400

By decoupling these models (e.g., Aiba combined with Monod, pH, and temperature factors), we balance biological realism and computational manageability, allowing focused evaluation of variables impacting cyanobacterial growth [12]. After establishing a biomass growth model, the PHB yield is analyzed by estimating the production rates and evaluating the impact of PHB consumption [14,15], providing a comprehensive view of bioplastic accumulation in response to environmental conditions. The complete expressions for each model mentioned are provided in Table 2.

2.2.2. Parameter estimation

Parameter estimation involves assigning values to model parameters to optimize the alignment between model predictions and experimental growth. Two methods were applied: (i) the *curve_fit* function from the *SciPy* library for nonlinear equations, and (ii) the *Pyomo* library, using a Concrete type model with 50 interior finite element discretization, the *piopt* solver, and mean squared error as the objective function for dynamic systems. Estimated parameter values were cross-referenced with ranges reported in the literature to ensure that the estimations are consistent with biological behaviors, thereby improving the model's reliability and interpretability.

2.2.3. Implementation

Each dataset was simulated separately using the models. Normalized Root Mean Square Error (NRMSE) was used to quantify the percentage error between simulated and experimental data [16]. NRMSE is calculated as follows, where y_i represents the experimentally measured biomass at time i, θ_i represents the biomass value predicted by the model at time i, N is the total number of data points, and $\hat{y}$ is the mean of the experimentally measured biomass values:

$$NRMSE = \frac{\sqrt{(\sum_{i=1}^{n}(y_i - \theta_i)^2/N)}}{\hat{y}}. \quad (1)$$

Each model was evaluated in two ways across datasets:

Table 2
Summary of growth models, including model name, mathematical expression, input variables, and estimated parameters.

Model	Expression	Variables	Parameters
Gompertz	$X(t) = X_0 \cdot \exp\left(-\exp\left(\mu \cdot e \cdot \frac{lag-t}{X_0} + 1\right)\right)$	X_0, t	$\mu,\ lag$
Baranyi-Roberts	$\frac{\partial X}{\partial t} = \mu \cdot \alpha(t) \cdot \left(1 - \frac{X}{X_{\max}}\right) \cdot X$	X_0	$\mu,\ X_{\max}$
Monod	$\frac{\partial X}{\partial t} = \mu \cdot \alpha(t) \cdot \frac{N}{N+K_N} \cdot X - \mu_d \cdot X^2$	$X_0,\ N$	$\mu,\ \mu_d,\ K_N$
Aiba	$\frac{\partial X}{\partial t} = \mu \cdot \alpha(t) \cdot \frac{I}{I+K_S+I^2/K_I} \cdot X - \mu_d \cdot X^2$	$X_0,\ I$	$\mu,\ \mu_d,\ K_S,\ K_I$
Lag phase	$\alpha(t) = \frac{a_0}{a_0+\exp(-\mu \cdot t)}$	t	a_0
pH	$\mu(\mathrm{pH}) = \frac{(\mathrm{pH}-\mathrm{pH}_M)(\mathrm{pH}-\mathrm{pH}_m)^2}{(\mathrm{pH}_o-\mathrm{pH}_m)[(\mathrm{pH}_o-\mathrm{pH}_m)(\mathrm{pH}-\mathrm{pH}_o)-(\mathrm{pH}_o-\mathrm{pH}_M)(\mathrm{pH}_o+\mathrm{pH}_m-2\mathrm{pH})]}$	pH	$\mathrm{pH}_{\mathrm{opt}},\ \mathrm{pH}_{\min},\ \mathrm{pH}_{\mathrm{Max}}$
T1	$\mu(T) = \frac{(T-T_M)\cdot(T-T_m)^2}{(T_o-T_m)\cdot[(T_o-T_m)\cdot(T-T_o)-(T_o-T_M)\cdot(T_o+T_m-2T)]}$	T	$T_{\mathrm{opt}},\ T_{\min},\ T_{\mathrm{Max}}$
T2 (Arrhenius)	$\mu(T) = \exp\left(-\frac{E_a}{R\cdot(T+273)} + \frac{E_a}{R\cdot T_a}\right)$	T	$\mu,\ \mu_d,\ E_a,\ T_a$
PHB production	$\mu(\mathrm{PHB}, t) = a \cdot X(t)$	X, t	a
PHB with degradation	$\mu(\mathrm{PHB}, t) = a \cdot X(t) - b$	X, t	$a,\ b$

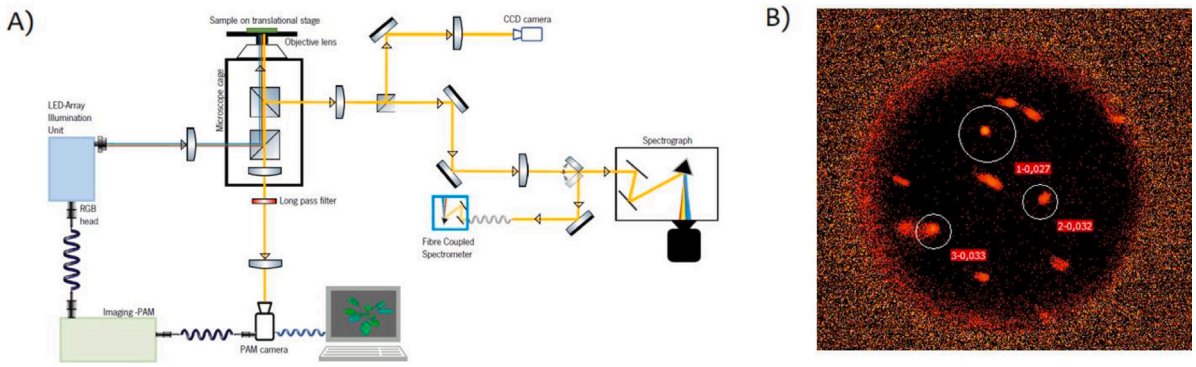

Fig. 2. (A) Setup of the optical system used for fluorescence measurement. (B) Fluorescence signals (red points), with points within the circle representing cyanobacteria selected for measurement.

- **Calibration.** For each experiment, the parameters are calibrated and the NRMSE is computed. The overall model calibration error is represented by the average NRMSE obtained from the calibration of each experiment.
- **Prediction.** Model parameters are estimated using all but one experiment, which is reserved as the validation set. The average of the estimated parameters is then calculated. The model is run for the environmental conditions of the validation experiment using the averaged parameters, and NRMSE is computed to assess predictive accuracy on the unseen data. This process is repeated, rotating through each experiment as the validation set, ensuring the independence of the results. The overall predictive performance of the model is quantified by the mean NRMSE across all experiments.

2.2.4. Sensitivy analysis

The effect of parameter fluctuations was studied by increasing and decreasing each parameter by a percentage of its original value while keeping all other parameters fixed at their optimized settings. We opted for a 1% variation in our study to focus on small fluctuations around the optimized parameter values [17]. The percentage change in the model output was then computed. This approach enables the identification of parameters that exert the most significant influence on the model's behavior and provides insight into the robustness of the model.

2.3. Photosynthetic activity monitoring

The PAM-FIS technique was used to assess photosynthetic activity [18]. The FIS method analyzes the Fourier transform of an image to extract spatial frequency content, while the PAM technique measures chlorophyll fluorescence changes in response to light intensity variations. Combined, these techniques provide both spatial and spectral photonic information, as well as photosynthetic activity at the micrometer scale. Experiments were conducted at the Nanophotonics Department of the Iberian Nanotechnology Laboratory (INL). The experimental setup is illustrated in Fig. 2. Over one month, 20 mL aliquots were sampled weekly from *Synechocystis sp.* strain and M8 microbiome cultures to assess photosynthetic efficiency as biomass increased. The maximum quantum yield (MQY), a key indicator of photosynthetic activity, was obtained through a sequence of light pulses applied to the fluorescence signals of the cyanobacteria.

3. Results and discussion

3.1. Model definition

The Gompertz and Baranyi-Roberts models were ineffective in accurately capturing cyanobacterial growth characteristics during both calibration and prediction in the three data sets. In contrast, models incorporating abiotic factors demonstrated superior performance. The Aiba model generally exhibited better predictive capabilities than the Monod model. Combining the Aiba model with temperature and pH resulted in a 65% reduction in NRMSE compared to the baseline Aiba model. Adding the Monod model in the combination ranked second in predictive accuracy, suggesting that future work should explore alternative nutrient-based models.

A significant reduction in fitting errors was observed as more calibration data became available, as demonstrated within Dataset 3 (Microbiomes - UPC). Additionally, predictive errors were much larger when calibration experiments showed greater differences between experimental conditions, as seen in Dataset 1 (Synechocystis - AIMEN). Fig. 3 illustrates the NRMSE values for calibration and simulation. The overall NRMSE for the coupled Aiba model with temperature and pH is 9.09% for calibration and 37.75% for prediction. These results align with those reported in the literature [7,13].

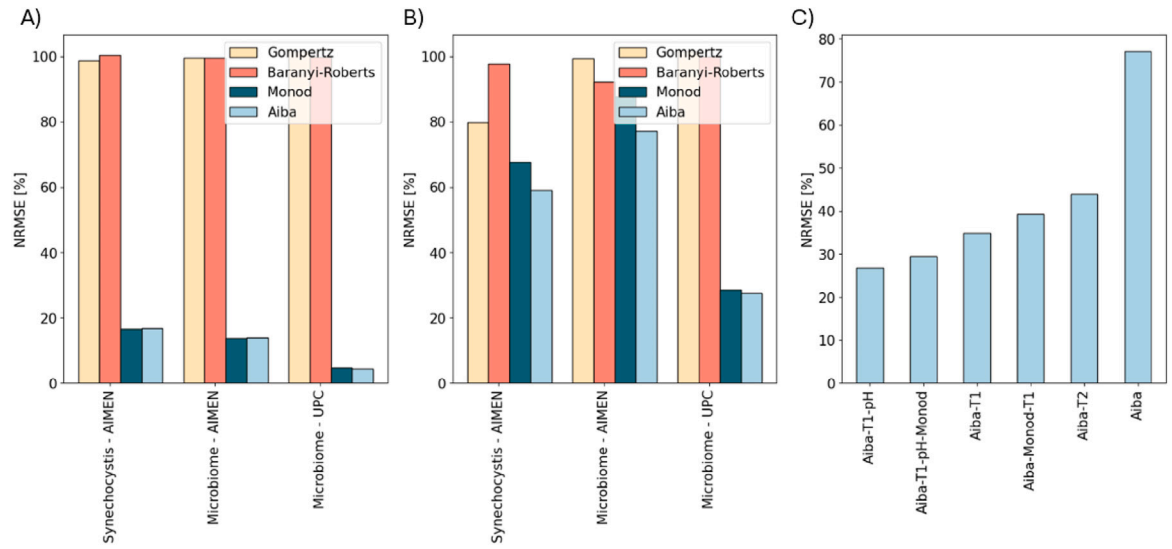

Fig. 3. NRMSE values for models in Table 2: (A) Calibration errors across the three datasets, (B) Simulation errors across the three datasets, and (C) Simulation errors for coupled Aiba model configurations on Dataset 2 (Microbiomes - AIMEN).

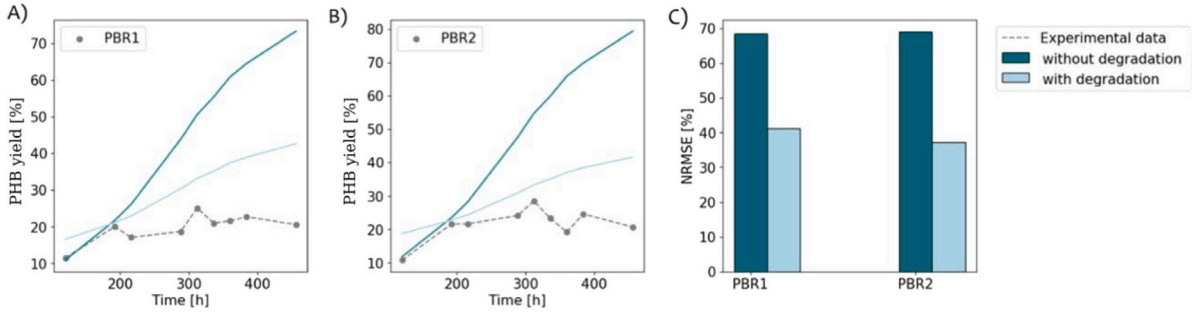

Fig. 4. Fitting of PHB models to experimental data: (A) PBR1, (B) PBR2, and (C) associated NRMSE values for the model fits.

Fig. 4 compares the effect of considering cellular PHB consumption in the estimation of PHB yield. Incorporating cyanobacterial degradation rates provides a more accurate reproduction of the percentage of PHB in the biomass achieved in each photobioreactor. However, the proposed model still exhibits a tendency to overestimate bioplastic production. This likely arises from the specific conditions required to trigger PHB accumulation, namely, a dark period and nutrient deprivation, while the biomass model used to estimate growth simulates standard growth conditions, lacking these stress factors. Furthermore, since PHB synthesis typically occurs once cell growth has decelerated, future improvements to the model should integrate the nutrient availability dynamics.

Based on these results, the following model is proposed to estimate biomass and analyze the amount of PHB that could be achieved in the estimated biomass:

$$\left.\begin{aligned}
\frac{\partial X}{\partial t} &= \mu \cdot \alpha(t) \cdot \mu(pH) \cdot \mu_{T1}(T) \cdot \frac{I}{I+K_S+I^2/K_I} \cdot X - \mu_d \cdot X^2, \\
\alpha(t) &= \frac{a_0}{a_0+\exp(-\mu t)}, \\
\mu(pH) &= \frac{(pH-pH_M)(pH-pH_m)^2}{(pH_o-pH_m)[(pH_o-pH_m)(pH-pH_o)-(pH_o-pH_M)(pH_o+pH_m-2pH)]} \\
\mu_{T1}(T) &= \frac{(T-T_M)\cdot(T-T_m)^2}{(T_o-T_m)\cdot[(T_o-T_m)\cdot(T-T_o)-(T_o-T_M)\cdot(T_o+T_m-2T)]} \\
PHB(t) &= a \cdot X(t) - b.
\end{aligned}\right\} \quad (2)$$

3.1.1. Parameter estimation

The parameter estimation analysis was conducted to evaluate the consistency and robustness of the developed model. Parameters for temperature and pH align with empirical findings from [7], specifically: $pH_{opt} = 8.52$, $pH_{min} = 3.9$, $pH_{max} = 13.08$, $T_{opt} = 32$ °C, $T_{min} = 15.57$ °C, and $T_{max} = 32$ °C. For the remaining seven parameters, estimated values across datasets and references can be found in Table 3.

Although some discrepancies arise between our estimates and those reported in the literature, they can be contextualized by the experimental framework used:

- Maximum Growth Rate (μ_{max}). Controls culture growth speed, with lower values indicating slower growth rates [22]. The estimated values for our model are well-aligned with those reported in the literature.
- Lag Phase Constant (a_0). Although the relationship between a_0 and adaptation duration is indirect, higher values suggest a more extensive adaptation requirement for the cells [23]. Estimations for a_0 are consistent with values in the literature.
- Decay Rate (μ_d). Represents the cell death rate. Estimated values are notably smaller than those in the literature. This discrepancy is due to the calibration experiments not reaching the cell death stage, rendering μ_d relatively inconsequential in this context [24].
- Light Saturation (K_S) and Inhibition Coefficients (K_I). Define optimal and harmful light intensities, respectively. Although references vary due to experimental conditions, our estimations for K_S and K_I are consistent across datasets with similar lighting. Notably, the K_I value of approximately 1300 $\mu molm^{-2}s^{-1}$ aligns with an irradiance level three times the applied intensity, consistent with ratios reported [13].
- PHB Accumulation Rate (a). Represents the rate at which biomass is accumulated as PHB. Our findings indicate a production rate

Table 3
Parameter estimation results: parameter expressions, literature values, and average estimates from experiments for each dataset.

Parameter	References	Dataset 1	Dataset 2	Dataset 3
$\mu[1/h]$	0.45 [12], 0.2 [7]	0.104	0.041	0.181
$\mu_d[g/Lh]$	0.02 [12], 1e-5 [19]	1e−05	8e−06	9e−02
$K_S[PPFD]$	165 (I=92) [13], 300 (I=20) [7]	633.33	400	535.871
$K_I[PPFD]$	457 (I=92) [13], 726 (I=100) [20]	1166.66	1333.33	1239.84
a_0	0.51 [21]	0.33	0.377	0.511

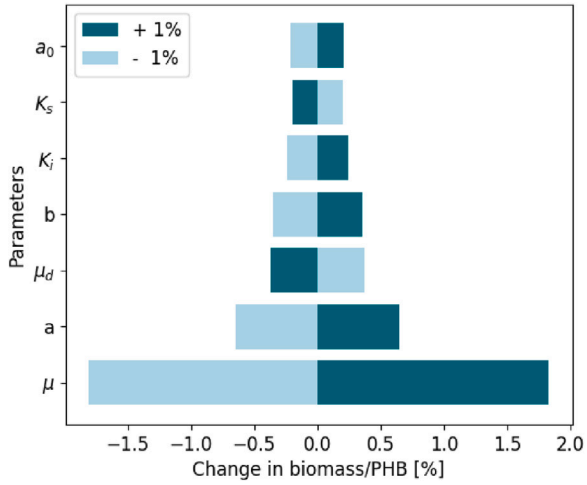

Fig. 5. Average sensitivities of model parameters to changes in input variables across all datasets.

of approximately 0.2, higher than the values typically reported in the literature [14]. This discrepancy likely arises from the overestimation of the model, previously discussed.

- PHB Degradation Rate (b). Reflects PHB degradation by the cells. No specific reference values for b were found in the literature for this parameter.

3.1.2. Sensitivity analysis

The impact of each parameter in the proposed model was evaluated through sensitivity analysis. The maximum growth rate, μ, emerged as the most sensitive parameter. A 1% increase in μ results in a 2% change in the biomass estimated. In contrast, parameters associated with environmental adaptation induce changes approximately five times smaller than those caused by variations in μ, suggesting that the model is more stable concerning environmental adaptation factors. This underscores the importance of accurately estimating the maximum growth rate, as it has a greater impact on the predicted biomass than other parameters. The results of the sensitivity analysis are presented in Fig. 5.

3.2. Optimization

A significant disparity in growth dynamics was observed across the datasets, which is reflected in both experimental observations and model predictions. Fig. 6 presents three representative samples of the experimental and simulated growth data.

The variation in the onset of growth was observed across the datasets, with significant differences in how quickly growth was initiated:

- In Dataset 2 (Microbiomes - AIMEN), the M8 microbiome experiment exhibited delayed growth initiation, captured by the model with a parameter $a_0 = 1$, indicating a substantial delay in growth compared to the other datasets.

Table 4
Comparison of experimental and model-optimized values: irradiance, achieved biomass, maximal PHB achievable.

	Irradiance [PPFD]		Biomass [mg/L]		PHB [mg/L]	
	Exp	Opt	Exp	Opt	Exp	Opt
M11 № 1	400	387	1204.49	1205.71	42.32	42.35
M11 № 2	400	387	1091.39	1093.16	39.61	39.65
M8	400	837	937.41	1367.76	34.42	40.82

- In contrast, the M11 microbiome in Dataset 2 (Microbiomes - AIMEN) demonstrated a much faster growth initiation, with a significantly lower a_0 value of 0.1.
- Dataset 3 (Microbiomes - UPC) showed a moderate delay in growth initiation, with an a_0 value of 0.5, consistent with the observed experimental trends. Dataset 1 (Synechocystis - AIMEN) also exhibited a moderate growth initiation delay, with an a_0 value of 0.3.

Differences in the overall growth rate across datasets were also noticed:

- Dataset 3 (Microbiomes - UPC) exhibited the fastest growth, reaching 1 gram of biomass in the shortest amount of time, with a predicted maximum growth rate (μ) of 0.181.
- Dataset 1 (Synechocystis - AIMEN) demonstrated a slower growth rate, with $\mu = 0.104$.
- Dataset 2 (Microbiomes - AIMEN), particularly the M8 microbiome, demonstrated the slowest growth, with the lowest estimated $\mu = 0.041$, indicating significant growth retardation compared to the other datasets.

Additionally, variations in biomass evolution under different light intensities were investigated, revealing notable differences for experiments corresponding to Dataset 2 (Microbiomes - AIMEN) (see Fig. 7).

Initially, biomass remains low across all irradiance values. As growth advances, light intensity plays a more significant role in biomass production. M11 cultures achieve higher biomass levels between 200 and 800 PPFD, with an optimal intensity at 387 PPFD, whereas M8 cultures peak between 500 and 1000 PPFD, reaching their optimum at 837 PPFD. Beyond optimal ranges, biomass declines, consistent with excessive light intensity causing cellular damage.

Comparisons between biomass and the amount of PHB that could be achieved in the estimated biomass, under optimal and experimental conditions, are summarized in Table 4. For M11 microbiomes, as the experimental conditions are already near optimal, further improvements at the optimal intensity are minimal, supporting the model's estimation of the optimal light conditions. In contrast, M8 microbiomes exhibit a significant increase in PHB content within the biomass, rising from 34.42 mg/L to 40.82 mg/L, representing a 18.59% increase when optimized. This suggests potential for further enhancement through light intensity adjustments. However, while the results indicate that light optimization can maximize biomass and PHB yield, the literature remains controversial [25], and further research is needed to substantiate this claim.

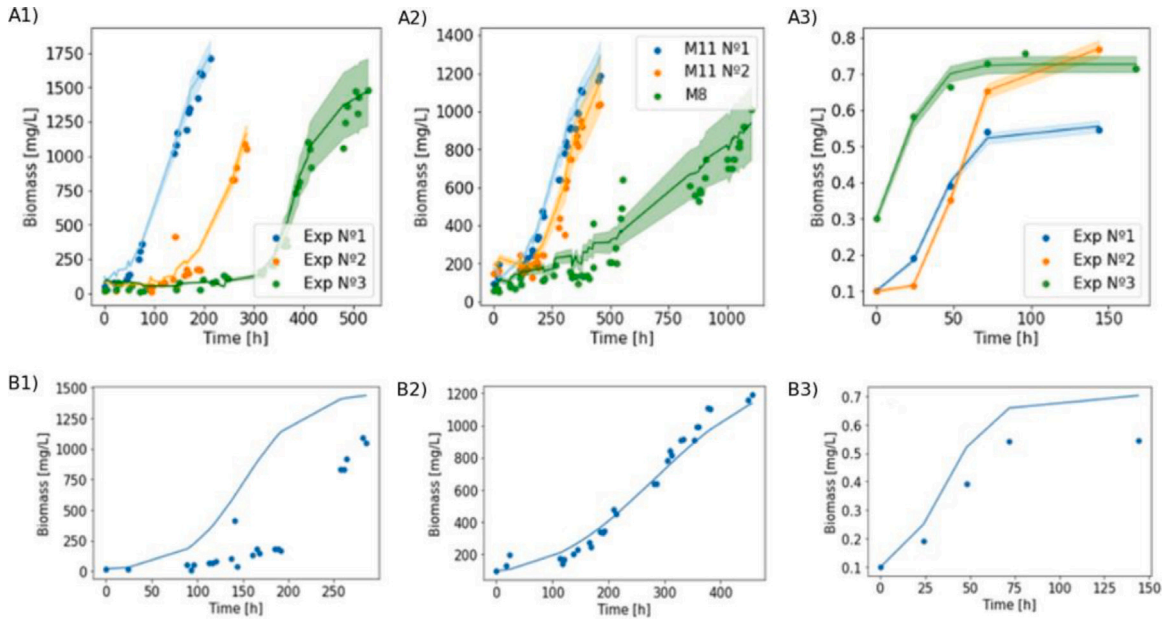

Fig. 6. Growth data for (1) Dataset 1 (Synechocystis - AIMEN), (2) Dataset 2 (Microbiome - AIMEN), and (3) Dataset 3 (Microbiomes - UPC) samples. (A) Model calibration and (B) model predictions for a specific experiment. Dots represent experimental data, while lines indicate model simulations.

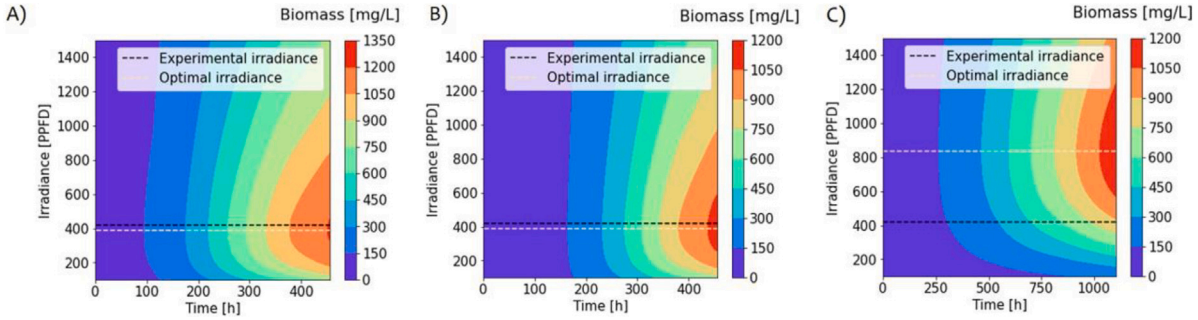

Fig. 7. Biomass distribution over time under varying irradiance for Dataset 2 (Microbiome - AIMEN): (A) Microbiome M11, Experiment 1, (B) Microbiome M11, Experiment 2, and (C) Microbiome M8.

3.3. Photosynthetic activity monitoring

Since photosynthesis drives light utilization, PAM-FIS measurements were conducted to correlate cyanobacterial photosynthetic activity with growth. For the *Synechocystis sp.* strain, three measurements were taken with dark adaptation (cyanobacteria kept in darkness for 20 min before light pulses) and two without. For the microbiome, two measurements were taken under light conditions and two in darkness. High p-values (see Table 5) indicated no significant difference in photosynthetic activity between dark-adapted and non-adapted cyanobacteria, consistent with previous research [26], which suggests cyanobacteria respond differently to dark adaptation than plant cells. Fluorescence signals were examined under red, blue, and green light, with successful detection only under red light. This corresponds to the absorption spectra of photosynthetic pigments in *Synechocystis sp.* and *Synechococcus sp.* (chlorophyll a, carotenoids, and phycobiliproteins), which predominantly absorb light in the 400–700 nm range [15]. While blue light is known to enhance phycocyanin production, red light appears more effective for overall photosynthetic activity.

MQY values ranged from 0.30 to 0.55 for pure cultures and microbiomes, aligning with literature values for healthy cells [27,28]. A negative Pearson's correlation of −0.88 between biomass and photosynthetic activity was observed (Fig. 8). This may be due to the increased opacity of cyanobacteria as biomass grows, which leads to light competition and reduced photosynthetic efficiency. At the same time, early cultures require optimized light capture for survival due to limited nutrient reserves. Diluting cultures as they grow may be beneficial, as it ensures cyanobacteria receive optimal light exposure, preventing a slowdown in photosynthetic activity and maintaining biomass productivity.

Table 5
P-values for comparing light adaptation (LA) and dark adaptation (DA) similarity between pure strain and microbiome samples.

		DA 1	DA 2	DA 3
Sy	LA 1	10.3%	92.16%	14.05%
Sy	LA 2	12.34%	2.03%	2.7%
M8	LA1	92.18%	5.2%	
M8	LA 2	0.90%	1.1%	

4. Conclusions

This study compared four growth models—Gompertz, Baranyi-Roberts, Monod, and Aiba—to evaluate the influence of various variables on growth dynamics. Empirical models failed to accurately capture cyanobacterial growth across the three datasets compiled in this study, emphasizing the need for abiotic models. Incorporating temperature and pH in the Aiba model notably improved accuracy, reducing

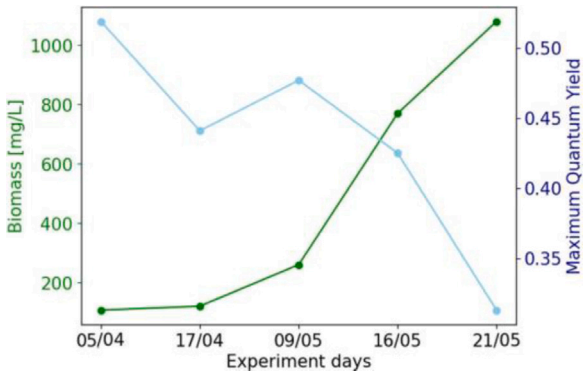

Fig. 8. Biomass versus photosynthetic activity: the blue line shows the photosynthetic activity trend, the green line represents the growth trend, and the dots correspond to experimental data for both parameters.

the NRMSE by 65% compared to the baseline. While the Monod-based variant also performed well, it was less accurate, suggesting further exploration of nutrient-based models. The parameter estimation analysis revealed the maximum growth rate as the most sensitive parameter, with a 1% increase resulting in a 2% change in biomass, while environmental adaptation parameters had a smaller effect.

An estimator for the achievable PHB yield within a given biomass was analyzed. Incorporating PHB degradation enhanced yield estimation, although the model still overestimated PHB production. Future work should consider stress factors and the timing of PHB synthesis in relation to growth phases to improve the accuracy of the estimator.

The model developed with irradiance, temperature, and pH achieved 90% accuracy in calibration and 63% in growth prediction, alongside a method to estimate PHB yield. It effectively captured variations in growth initiation and rates, with higher μ values indicating faster growth and higher a_0 values reflecting slower growth onset. Optimizing light intensity showed potential for increasing PHB content, especially for the M8 microbiome, with a predicted 18.59% increase, while confirming optimal conditions for the other experiments. These findings suggest that adjusting light intensity could enhance biomass and PHB production, though further research is needed due to inconsistencies in the literature. PAM-FIS experiments showed red light as more efficient for overall photosynthetic activity and revealed a negative correlation between growth and photosynthetic efficiency. This suggests that diluting the culture as it grows could optimize light exposure, maximizing biomass productivity. Using a red light filter may further enhance biomass growth efficiency.

In conclusion, this study offers a framework for estimating biomass accumulation in response to environmental variables, particularly focusing on light. The findings provide valuable insights for optimizing laboratory conditions and defining the ideal environmental factors at each growth stage to enhance biocompound production. Expanding calibration data is essential for improving the model's accuracy, and incorporating more precise representations of nutrient consumption could further optimize it. By deepening our understanding of these factors, we can establish more effective guidelines for controlling PHB production, paving the way for sustainable bioplastic and bioproduct development.

CRediT authorship contribution statement

I. Perez Couñago: Writing – review & editing, Writing – original draft, Visualization, Validation, Software, Methodology, Investigation, Formal analysis, Data curation, Conceptualization. **J.M. Fernandez Montenegro:** Writing – review & editing, Validation, Supervision, Data curation, Conceptualization. **S. Iglesias Moreira:** Writing – review & editing, Validation, Supervision, Project administration, Funding acquisition, Data curation, Conceptualization. **F. Rodriguez Lorenzo:** Validation, Conceptualization. **M. Placer Lorenzo:** Validation. **P. Villar Sola:** Data curation. **E. Pancorbo González:** Data curation. **J. Illade Quinteiro:** Project administration. **L. Herrero Castilla:** Project administration. **J.A. Álvarez Rodríguez:** Project administration. **B. Altamira Algarra:** Data curation. **E. Gonzalez Flo:** Data curation. **J. Garcia:** Data curation. **F. Guedes:** Data curation. **M. Lopez-Garcia:** Data curation. **S. Muiños-Landin:** Writing – review & editing, Visualization, Validation, Supervision, Project administration, Methodology, Data curation.

Declaration of Generative AI and AI-assisted technologies in the writing process

During the preparation of this work, the author(s) used ChatGPT to improve language and readability. After using this tool/service, the author(s) reviewed and edited the content as needed and take(s) full responsibility for the content of the publication.

Declaration of competing interest

The authors declare the following financial interests/personal relationships which may be considered as potential competing interests: Ines Perez reports financial support was provided by AIMEN Technology Centre. Ines Perez reports a relationship with Horizon 2020 European Innovation Council Fast Track to Innovation, under grant agreement No 10100073, that includes: funding grants. If there are other authors, they declare that they have no known competing financial interests or personal relationships that could have appeared to influence the work reported in this paper.

Acknowledgments

This work was funded by the European Union's Horizon 2020 research and innovation program under grant agreement No 101000733 (PROMICON project).

References

[1] Cox KD, Covernton GA, Davies HL, Dower JF, Juanes F, Dudas SE. Human consumption of microplastics. Environ Sci Technol 2019;53(12):7068–74.
[2] Han SF, Jin WB, Tu RJ, Wu WM. Biofuel production from microalgae as feedstock: current status and potential. Crit Rev Biotechnol 2015;35(2):255–68.
[3] Alsabri A, Tahir F, Al-Ghamdi SG. Environmental impacts of polypropylene (PP) production and prospects of its recycling in the GCC region. Mater Today: Proc 2022;56:2245–51.
[4] Parmar A, Singh NK, Pandey A, Gnansounou E, Madamwar D. Cyanobacteria and microalgae: a positive prospect for biofuels. Bioresour Technol 2011;102(22):10163–72.
[5] Rueda E, García-Galán MJ, Díez-Montero R, Vila J, Grifoll M, García J. Polyhydroxybutyrate and glycogen production in photobioreactors inoculated with wastewater borne cyanobacteria monocultures. Bioresour Technol 2020;295:122233.
[6] American Public Health Association, American Water Works Association. Standard methods for the examination of water and wastewater. 1995, 1000–1000.
[7] Rueda E, García J. Optimization of the phototrophic cyanobacteria polyhydroxybutyrate (PHB) production by kinetic model simulation. Sci Total Environ 2021;800:149561.
[8] Altamira-Algarra B, Lage A, Meléndez AL, Arnau M, Gonzalez-Flo E, García J. Bioplastic production by harnessing cyanobacteria-rich microbiomes for long-term synthesis. Sci Total Environ 2024;954:176136.
[9] Lanham AB, Ricardo AR, Albuquerque MGE, Pardelha F, Carvalheira M, Coma M, et al. Determination of the extraction kinetics for the quantification of polyhydroxyalkanoate monomers in mixed microbial systems. Process Biochem 2013;48:1626–34. http://dx.doi.org/10.1016/j.procbio.2013.07.023.
[10] Winsor CP. The Gompertz curve as a growth curve. Proc Natl Acad Sci 1932;18(1):1–8.
[11] Muloiwa M, Nyende-Byakika S, Dinka M. Comparison of unstructured kinetic bacterial growth models. South Afr J Chem Eng 2020;33:141–50.

[12] Zhang D, Dechatiwongse P, Del-Rio-Chanona EA, Hellgardt K, Maitland GC, Vassiliadis VS. Analysis of the cyanobacterial hydrogen photoproduction process via model identification and process simulation. Chem Eng Sci 2015;128:130–46.
[13] Zhang D, Dechatiwongse P, del Rio-Chanona EA, Maitland GC, Hellgardt K, Vassiliadis VS. Modelling of light and temperature influences on cyanobacterial growth and biohydrogen production. Algal Res 2015;9:263–74.
[14] Carpine R. Cyanobacteria for PHB production. R. Carpine, Discussion of PHB Production. 2018, p. 84–5.
[15] Whitton BA, Potts M. Introduction to the cyanobacteria. In: Ecology of cyanobacteria II: their diversity in space and time. 2012, p. 1–13.
[16] Shcherbakov MV, Brebels A, Shcherbakova NL, Tyukov AP, Janovsky TA, Kamaev VAE. A survey of forecast error measures. World Appl Sci J 2013;24(24):171–6.
[17] Rabitz H, Kramer M, Dacol D. Sensitivity analysis in chemical kinetics. Annu Rev Phys Chem 1983;34(1):419–61.
[18] Wardley WP, Goessling JW, Lopez-Garcia M. Measuring photonics in photosynthesis: Combined micro-Fourier image spectroscopy and pulse amplitude modulated chlorophyll fluorimetry at the micrometre-scale. Biomimetics 2022;7(3):107.
[19] Guven B, Howard A. Modelling the growth and movement of cyanobacteria in river systems. Sci Total Environ 2006;368(2–3):898–908.
[20] Krichen E, Rapaport A, Le Floc'h E, Fouilland E. A new kinetics model to predict the growth of micro-algae subjected to fluctuating availability of light. Algal Res 2021;58:102362.
[21] Ortiz-Moreno ML, Cárdenas-Poblador J, Agredo J, Solarte-Murillo LV. Modeling the effects of light wavelength on the growth of Nostoc ellipsosporum. Univ Sci 2020;25(1):113–48.
[22] Maier RM, Pepper IL. Bacterial growth. In: Environmental microbiology. Academic Press; 2015, p. 37–56.
[23] Swinnen IAM, Bernaerts K, Dens EJ, Geeraerd AH, Van Impe JF. Predictive modelling of the microbial lag phase: a review. Int J Food Microbiol 2004;94(2):137–59.
[24] Novick A, Szilard L. Description of the chemostat. Science 1950;112(2920):715–6.
[25] Gracioso LH, Bellan A, Karolski B, Cardoso LOB, Perpetuo EA, do Nascimento CAO, et al. Light excess stimulates poly-beta-hydroxybutyrate yield in a mangrove-isolated strain of synechocystis sp. Bioresour Technol 2021;320:124379.
[26] Schuurmans RM, van Alphen P, Schuurmans JM, Matthijs HC, Hellingwerf KJ. Comparison of the photosynthetic yield of cyanobacteria and green algae: different methods give different answers. PLoS One 2015;10(9):e0139061.
[27] Ogawa T, Misumi M, Sonoike K. Estimation of photosynthesis in cyanobacteria by pulse-amplitude modulation chlorophyll fluorescence: problems and solutions. Photosynth Res 2017;133:63–73.
[28] Acuna AM, Snellenburg JJ, Gwizdala M, Kirilovsky D, van Grondelle R, van Stokkum IH. Resolving the contribution of the uncoupled phycobilisomes to cyanobacterial pulse-amplitude modulated (PAM) fluorometry signals. Photosynth Res 2016;127:91–102.